

# Optimal Power Allocation for OFDMA Systems under I/Q Imbalance

Alexandros – Apostolos A. Boulogeorgos, *Student Member, IEEE*,

Panagiotis D. Diamantoulakis, *Student Member, IEEE*, and George K. Karagiannidis, *Fellow, IEEE*

**Abstract**—Direct-conversion architectures can offer highly integrated low-cost hardware solutions to communication transceivers. However, it has been demonstrated that radio frequency (RF) impairments, such as amplifier nonlinearities, phase noise and in-phase/quadrature-phase imbalances (IQI), can lead to a severe degradation in the performance and fairness. To this end, we study the power allocation (PA) problem in an orthogonal frequency-division multiple access (OFDMA) system, when the served user equipments (UEs) suffer from different levels of IQI. Additionally, we present a novel low-complexity solution with directly calculated PA policies, given the Lagrange multiplier, which mitigates the impact of IQI and achieves fairness in terms of capacity for the served UEs, by maximizing the minimum achievable capacity of the UEs. The effectiveness of the offered solution is validated through simulation results, which reveal that it can drastically increase the minimum achievable UEs' capacity.

**Index Terms**—Fairness, Hardware-constrained communications, I/Q imbalance, Multi-carrier communications, OFDMA, Power allocation.

## I. INTRODUCTION

THE ever-increasing demand for high data rate applications and multimedia services has led to the development of flexible and software-configurable transceivers that are capable of supporting the desired quality of service requirements. In this context, direct-conversion architecture provides an attractive front-end solution, as it requires neither external intermediate frequency filters nor image rejection filters. Instead, the essential image rejection is achieved through signal processing methods. Direct-conversion architectures are low cost and can be easily integrated on chip, which render them excellent candidates for modern wireless technologies [1], [2]. However, they are typically sensitive to front-end radio frequency (RF) impairments, which are often inevitable due to components mismatch and manufacturing defects [3]–[7]. An indicative example is the in-phase (I) and quadrature (Q) imbalance (IQI), which corresponds to the amplitude and phase mismatch between the I and Q branches of a transceiver and ultimately leads to imperfect image rejection that incurs

considerable performance degradation [8], [9]. Furthermore, in multicarrier systems, IQI creates an additional image-signal from the mirror subcarrier, which leads to a throughput ceiling [10].

Various approaches have been proposed so far to eliminate, compensate, and mitigate the effects of IQI using baseband signal processing techniques at the receiver (RX) (see [11]–[15], and references therein). For example, in [11], the authors presented an IQI mitigation method for orthogonal frequency division multiple access (OFDMA) systems, in which each subcarrier is processed jointly with its counterpart at the image subcarrier. All previously mentioned works deal with IQI at the RX by employing digital signal processing. However, in wireless systems, where low-cost, energy efficiency, low-complexity, and compactness of the RXs are key design requirements, the extra processes in the RX may be prohibitive. Motivated by this, in the present work, we investigate the power allocation (PA) problem for OFDMA wireless systems, when the served user equipments (UEs) suffer from different levels of IQI. To take into consideration the impact of IQI, we propose a novel low-complexity solution with directly calculated PA policies, given the Lagrange multiplier, that maximizes the minimum UEs' achievable capacity, with respect to the base station (BS) transmitted power. The proposed PA solution outperforms the conventional one, which does not take into consideration the IQI levels of the served UEs, while, at the same time, fairness in terms of capacity of the served UEs is achieved. The effectiveness of the offered solution is validated through simulations, which reveal that it can significantly increase the minimum achievable UEs' capacity.

*Notations:* Unless otherwise stated,  $(\cdot)^*$  denotes conjugation, whereas  $\Re\{x\}$  and  $\Im\{x\}$  represent the real and imaginary part of  $x$ , respectively. Furthermore, the  $\mathbb{E}[\cdot]$  and  $|\cdot|$  operators denote statistical expectation and absolute value operations, respectively.

## II. SYSTEM AND SIGNAL MODEL

In this section, we revisit the ideal signal model, as well as the realistic IQI signal models in multi-carrier direct-conversion RX scenario in an OFDMA system.

### A. Ideal RF front-end

We assume OFDMA transmission, where a transmitted signal at subcarrier  $k$  for the UE  $i$ ,  $s_i(k)$ , conveyed over a wireless channel,  $h_i(k)$ , with an additive white Gaussian noise

The authors are with the Department of Electrical and Computer Engineering, Aristotle University of Thessaloniki, 54 124, Thessaloniki, Greece (e-mail: {ampoulog, padiaman, geokarag}@auth.gr).

Copyright (c) 2015 IEEE. Personal use of this material is permitted. However, permission to use this material for any other purposes must be obtained from the IEEE by sending a request to pubs-permissions@ieee.org.

Manuscript received xxxxxx; revised xxxxxx; accepted xxxxxx. Date of publication xxxxx, xx xxxx; date of current version xxxxx, xx xxxx. The associate editor coordinating the review of this paper and approving it for publication was xxxxxx.

Digital Object Identifier xxxxxx

(AWGN),  $n_i(k)$ . The received RF signal is passed through various processing stages, also known as the RF front-end of the RX. These stages include filtering, amplification, analog I/Q demodulation, down-conversion to baseband and sampling. To this end, the corresponding baseband equivalent received signal can be expressed as  $r_{\text{id},i}(k) = h_i(k)s_i(k) + n_i(k)$ . Note that  $h_i(k)$  is given by  $h_i(k) = \frac{g_i(k)}{D_i^n}$ , where  $g_i(k)$  is a complex Gaussian random variable,  $n$  represents the path loss exponent and  $D_i = \frac{d_i}{d_0}$ , with  $d_i$  and  $d_0$  be the distance between the BS and the  $i$ -th UE, and the reference distance, respectively. Based on this, the instantaneous signal to noise ratio (SNR) per symbol at the RX input of the  $i$ -th UE can be given by,  $\gamma_{\text{id},i}(k) = \frac{P_s(k)}{N_0} |h_i(k)|^2$ , where,  $P_s(k)$ , denotes the power per transmitted symbol at subcarrier  $k$  and  $N_0$  is the single-sided AWGN power spectral density (PSD).

### B. I/Q imbalance Model

The time-domain baseband representation of the IQI impaired signal at the  $i$ -th UE is given by [1]  $g_i^{\text{no}} = K_{1,i}g_i + K_{2,i}g_i^*$ , where  $g_i$  denotes the baseband IQI-free signal at the  $i$ -th UE and  $g_i^*$  raised due to the involved IQI effects. Furthermore, the IQI coefficients  $K_{1,i}$  and  $K_{2,i}$  are expressed as  $K_{1,i} = \frac{1}{2}(1 + \epsilon_i e^{-j\theta_i})$  and  $K_{2,i} = \frac{1}{2}(1 - \epsilon_i e^{j\theta_i})$ , where  $\epsilon_i$  and  $\theta_i$  account for the RX amplitude and phase mismatch, of the  $i$ -th UE, respectively. It is also noted that the IQI parameters are algebraically linked to each other as  $K_{2,i} = 1 - (K_{1,i})^*$ . The  $K_{1,i}$  and  $K_{2,i}$  coefficients are associated with the corresponding image rejection ratio (IRR), which determines the amount of attenuation of the image frequency band and is expressed as  $\text{IRR}_i = \frac{|K_{1,i}|^2}{|K_{2,i}|^2}$ .

It is recalled here that for practical analog RF front-end electronics, the value of IRR is typically in the range of 20 dB – 40 dB [5], [16]–[18]. Furthermore, the second term,  $K_{2,i}g_i^*$ , is due to the associated imbalances and in multi-carrier transmission it denotes the image *aliasing* effect, which results to crosstalk between the mirror-frequencies in the down-converted signal. This is because, in general, complex conjugate in time domain corresponds to complex conjugate and mirroring in the frequency domain. Therefore, the spectrum of the imbalance signal at the  $k$ -th subcarrier becomes

$$G_{\text{IQI},i}(k) = K_{1,i}G_i(k) + K_{2,i}G_i^*(-k), \quad (1)$$

where  $G_i(k)$  and  $G_i(-k)$  denote the spectrum of the IQI free signal at the  $k$  and  $-k$  subcarriers, respectively. Note that in this paper, we assume frequency-independent IQI; however, the generalization to the frequency-dependent case is straightforward using the methodology in [19].

### C. OFDMA systems impaired by IQI

In the case of multi-user transmission, we assume that multiple RF subcarriers are down-converted to the baseband by means of wideband direct-conversion, where the RF spectrum is translated to the baseband in a single down-conversion. Note that the wideband conversion is the most general scenario in multi-carrier wireless systems [6]. For notational convenience, we denote the set of subcarriers/UEs

as  $\mathcal{K} = \{-K, \dots, -1, 1, \dots, K\}$ . Without loss of generality, it is assumed that the signal carried by the  $k$ -th subcarrier is intended for the  $k$ -th UE, a signal carried by the mirror subcarrier,  $-k$ , is intended for UE  $-k$ . Moreover, since the BS is usually a high-complexity device, the RF front-end of the TX is considered ideal, while the RX experiences IQI. Hence, by using (1), the baseband equivalent received signal in the  $k$ -th subcarrier of the  $i$ -th UE can be represented as

$$r_i(k) = K_{1,i}h_i(k)s_i(k) + K_{2,i}h_i^*(-k)s_{-i}^*(-k) + K_{1,i}n_k(k) + K_{2,i}n_k^*(-k), \quad (2)$$

while the baseband equivalent received signal in the  $-k$ -th subcarrier at the  $-i$ -th UE can be expressed as

$$r_{-i}(-k) = K_{1,-i}h_{-i}(-k)s_{-i}(-k) + K_{2,-i}h_{-i}^*(k)s_i^*(k) + K_{1,-i}n_{-i}(-k) + K_{2,-i}n_{-i}^*(k). \quad (3)$$

With the aid of (3), it is shown that IQI is the reason that the received baseband equivalent signal intended for the  $i$ -th UE,  $s_i(k)$ , (with  $i = k \in \mathcal{K}$ ) is interfered by the image signal intended for UE  $-i$ ,  $s_{-i}^*(-k)$ . The instantaneous signal to interference plus noise ratio (SINR) per symbol at the input of the RX of the  $i$ -th UE at subcarrier  $k$  can be expressed as

$$\gamma_i(k) = \frac{|h_i(k)|^2 P_s(k)}{\frac{|h_i(-k)|^2}{\text{IRR}_k} P_s(-k) + \left(1 + \frac{1}{\text{IRR}_i}\right) N_0}. \quad (4)$$

Similarly, the instantaneous SINR per symbol at the input of the RX of the  $-i$ -th UE can be obtained by interchanging  $i$  with  $-i$  and  $k$  with  $-k$  and vice versa in (4). Consequently, the achievable rates at UE  $i$ , with  $i = k \in \mathcal{K}$ , can be obtained as

$$R_i(k) = \log_2(1 + \gamma_i(k)). \quad (5)$$

## III. PROBLEM FORMULATION & PROPOSED PA SCHEME

In this section, we first define the PA optimization problem, and then, we present a novel solution. We consider that the optimization is performed by the BS, which has full channel state information (CSI)<sup>1</sup> as well as the served UEs IRR values of the served devices, which are reported to the BS by the UEs through a feedback channel, when they enter the wireless system. As we are interested in increasing the achievable capacity of each UE, we aim to maximize the minimum capacity with respect to the transmitted power. The corresponding optimization problem can be written as

$$\begin{aligned} \max_{\mathbf{P}} \quad & \min_{k \in \mathcal{K}} R_k \\ \text{s.t.} \quad & \text{C1: } \sum_{k \in \mathcal{K}} P_s(k) \leq P_{\max}, \end{aligned} \quad (6)$$

where  $\mathbf{P} = [P_s(-K), \dots, P_s(-1), P_s(1), \dots, P_s(K)]$  and  $P_{\max}$  stands for the maximum allowable transmitted power. The optimization problem in (6) corresponds is identical to

<sup>1</sup>Note that in practice, this can be achieved by estimating the channels at the BS, if the channel reciprocity property is valid, i.e. uplink and downlink occurs within a coherence block [20].

the problem of minimum SINR maximization, and, thus, it can be rewritten as

$$\begin{aligned} \max_{\mathbf{P}} \quad & \min_{k \in \mathcal{K}} \gamma_k \\ \text{s.t.} \quad & C_1 : \sum_{k \in \mathcal{K}} P_s(k) \leq P_{\max}, \end{aligned} \quad (7)$$

The objective function in (7) is not a purely analytical expression. However, by using the epigraph representation of the optimization problem in (6), it can be equivalently expressed as

$$\begin{aligned} \max_{\mathbf{P}} \quad & \mathcal{R} \\ \text{s.t.} \quad & C_1 : \sum_{k \in \mathcal{K}} P_s(k) \leq P_{\max}, \\ & C_2 : \gamma_k \geq \mathcal{R}, \forall k \in \mathcal{K}. \end{aligned} \quad (8)$$

In the above,  $C_2$  represents the hypograph of the original optimization problem in (6), with  $\mathcal{R}$  being an extra auxiliary variables.

Notice that the optimization problem in (8) is non-convex. However, it can be easily transformed into a convex one by replacing  $P_s(k)$  with  $\exp(x(k))$  and  $\mathcal{R}$  with  $\exp(y)$  and by following similar steps as in [21]. After some mathematical manipulations, this problem can be finally expressed as

$$\begin{aligned} \max_{\mathbf{P}} \quad & y \\ \text{s.t.} \quad & C_1 : \sum_{k \in \mathcal{K}} \exp(x(k)) \leq P_{\max}, \\ & C_2 : \ln \left( \frac{|h_k(-k)|^2}{\text{IRR}_k} \exp(x(-k) - x(k)) \right) \\ & \quad + \left( 1 + \frac{1}{\text{IRR}_k} \right) N_0 \exp(-x(k)) \\ & \quad + y - \ln \left( |h_k(k)|^2 \right) \leq 0, \forall k \in \mathcal{K}. \end{aligned} \quad (9)$$

Apparently, the constraint  $C_1$  is convex as a summation of convex functions, while  $C_2$  is also convex, because, its Hessian matrix has non-negative eigenvalues, given in (10), at the top of the next page. Consequently, the problem in (9) can be solved by using convex optimization techniques. Next, we solve it by using the dual decomposition method [22]. For this reason, the Lagrangian of (9) is needed, which can be obtained as [23]

$$\begin{aligned} L = & y - \lambda \left( \sum_{k \in \mathcal{K}} \exp(x(k)) - P_{\max} \right) \\ & - \sum_{k \in \mathcal{K}} \mu_k \left( \ln \left( \frac{|h_k(-k)|^2}{\text{IRR}_k} \exp(x(-k) - x(k)) \right) \right. \\ & \left. + \left( 1 + \frac{1}{\text{IRR}_k} \right) N_0 \exp(-x(k)) + y - \ln \left( |h_k(k)|^2 \right) \right), \end{aligned} \quad (11)$$

where  $\lambda \geq 0$  and  $\mu_k \geq 0$  are the Lagrange multipliers (LMs).

For fixed LMs, the optimal solution for  $x(k)$  and  $x(-k)$ , or equivalently for  $P_s(k)$  and  $P_s(-k)$ , are respectively obtained

by using the Karush-Kuhn-Tucker conditions as

$$\begin{aligned} \tilde{P}_s(k) = & -\frac{\xi_k}{2} + \frac{\mu_{-k} - \mu_k}{2\lambda} \\ & + \sqrt{\frac{\xi_k^2}{4} + \frac{(\mu_{-k} - \mu_k)^2}{4\lambda^2} + \frac{\xi_k}{2\lambda}(\mu_{-k} + \mu_k)}. \end{aligned} \quad (12)$$

where the coefficients  $\xi_k = (\text{IRR}_k + 1) \frac{N_0}{|h_{-k}(k)|^2}$ .

For given LMs, (12) is low-complexity directly calculated PA optimization solution, given the Lagrange multiplier, that can be calculated in parallel for each UE. Interestingly, it takes into consideration the RXs non-ideal characteristics and guarantees fairness in terms of UE achievable capacity. Additionally, we point out that, according to (12), the power allocated to the UE  $k$  is dependent from the RF characteristics and the channels of all the  $2K$  UEs that are served via the LMs,  $\lambda$  and  $\mu_k$ . Note that for  $K_{1,k} = 1$  and  $K_{2,k} = 0$  ( $k \in \{-K, \dots, -1, 1, \dots, K\}$ ), the proposed optimization solution is simplified to the PA for an ideal RF front-end scheme. This PA is used by the BS that is unaware of the UEs' RF imperfections, and to what follows, we refer to as "classical PA" [22]. The constants  $\lambda$  and  $\mu_k$  can be easily estimated, in polynomial time, by an iterative algorithm such as subgradient method, which is out of the scope of the current paper. Interested readers are referred to [23], [24] for further information.

**Proposition 1.** *The minimum achievable capacity is maximized when the inequality constraint in (6) is satisfied with equality.*

*Proof:* This can be straightforwardly proven by following the same steps as Corollary 1 in [25]. ■

**Proposition 2.** *At the optimal, the  $k$  and  $-k$  UEs will have the same achievable capacity.*

*Proof:* This can be straightforwardly proven by following the same steps as Corollary 2 in [25]. ■

#### IV. NUMERICAL RESULTS & DISCUSSION

In this section, we demonstrate the efficiency of the proposed PA scheme by presenting simulation results. In particular, we consider that a BS serves  $2K$  UEs. Each UE suffers from different levels of IQI. Furthermore, it is important to note that, unless otherwise is stated, in the following figures, we consider that  $n = 3$ ,  $\theta_k = 3^\circ$ ,  $\epsilon_k < 1$  and  $D_k = 1$  for  $k \in \mathcal{K}$ . Finally, without loss of generality, we assume that  $P_{\max} = 1$ .

Fig. 1 illustrates the detrimental effects of IQI on the achievable capacity of each UE and the efficiency of the proposed PA scheme. We observe that for low  $\frac{P_{\max}}{N_0}$  values, IQI does not affect the UEs capacity performance. However, as  $\frac{P_{\max}}{N_0}$  increases, the impact of IQI has adverse effects on its UEs achievable capacity. Furthermore, it is evident that the proposed PA scheme can mitigate the performance degradation, due to IQI and positively contribute to the increase of the UEs achievable capacity. For example, for  $\frac{P_{\max}}{N_0} = 35$  dB,  $\text{IRR}_1 = \text{IRR}_{-1} = 20$  dB, the use of the proposed PA scheme increases the average achievable rate about 22.3%.

$$\phi_1 = \frac{|h_k(-k)|^2 (1 + \text{IRR}_k) N_0 \exp(x(-k))}{\left( (1 + \text{IRR}_k) N_0 + |h_k(-k)|^2 \exp(x(-k)) \right)^2} \geq 0, \quad \phi_2 = 0, \quad \phi_3 = 0. \quad (10)$$

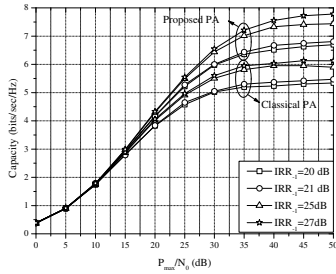


Fig. 1: Capacity as a function of  $\frac{P_{\max}}{N_0}$  for different levels of  $\text{IRR}_{-1}$ , when  $\text{IRR}_1 = 20$  dB and  $K = 1$ .

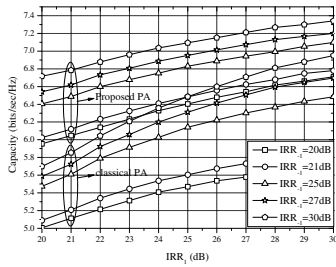


Fig. 2: Capacity as a function of  $\text{IRR}_1$  for different levels of  $\text{IRR}_{-1}$ ,  $\frac{P_{\max}}{N_0} = 30$  dB and  $K = 1$ .

This indicates the importance of taking into consideration the effects of the UEs IQI, when designing a PA scheme.

In Fig. 2, the UEs capacity as a function of the  $\text{IRR}_1$ , for different values of  $\text{IRR}_{-1}$  and  $\frac{P_{\max}}{N_0} = 30$  dB for both classical and the proposed PA schemes, is plotted. From this figure, it is evident that the proposed PA scheme outperforms the classical one for all the  $\text{IRR}_{-1}$  values. Moreover, it is observed that, for a given  $\text{IRR}_{-1}$ , as  $\text{IRR}_1$  increases, the signal leakage of the mirror subcarrier decreases; hence, the performance of the proposed PA scheme tends to those of the conventional scheme. For example, for  $\text{IRR}_{-1} = 30$  dB, for  $\text{IRR}_1 = 20$  dB, the use of the proposed PA scheme increases the average achievable rate about 18%, whereas for  $\text{IRR}_1 = 30$  dB and the same  $\text{IRR}_{-1}$ , the increase of the average achievable rate is about 5.6%.

In Fig. 3, the average achievable capacity of each UE of the proposed PA scheme as a function of  $\frac{P_{\max}}{N_0}$  for different values of  $K$  is depicted, when  $\text{IRR}_k = 20$  dB, with  $k \in \mathcal{K}$ . Again, it is observed that the proposed PA scheme outperforms the classical PA scheme for any value of  $K$  and in all the  $\frac{P_{\max}}{N_0}$  regime. Furthermore, from this figure, it is evident that as  $K$  increases, the effects of IQI become more detrimental. For instance, for  $K = 2$ , in the high  $\frac{P_{\max}}{N_0}$  regime, each UE capacity is limited to 4.21 bits/sec/Hz, while for  $K = 3$ , it is constrained to 3.63 bits/sec/Hz. Additionally, we observe that as  $K$  increases, the effectiveness of the proposed PA scheme increases. For example, for  $\frac{P_{\max}}{N_0} = 40$  dB, the use

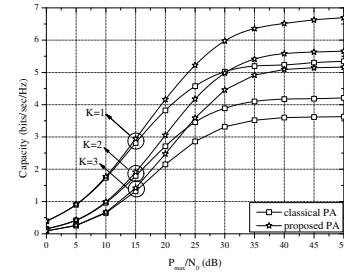


Fig. 3: Capacity as a function of  $\frac{P_{\max}}{N_0}$  for  $\text{IRR}_1 = \text{IRR}_{-1} = 20$  dB and different values of  $K$ .

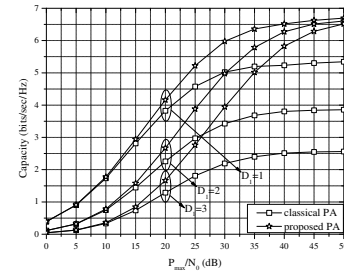


Fig. 4: Capacity as a function of  $\frac{P_{\max}}{N_0}$  for  $\text{IRR}_1 = \text{IRR}_{-1} = 20$  dB,  $K = 1$ ,  $D_{-1} = 1$  and different values of  $D_1$ .

of the proposed PA scheme results to 24.47%, 33.79% and 41.36% increase of the average UE capacity for  $K = 1$ ,  $K = 2$  and  $K = 3$ , respectively.

In Fig. 4, the average achievable capacity of each UE as a function of  $\frac{P_{\max}}{N_0}$  for different values of  $D_1$ , when  $K = 1$ ,  $D_{-1} = 1$ , and  $\text{IRR}_1 = \text{IRR}_{-1} = 20$  dB, is plotted. From this figure, it is evident that the proposed PA scheme outperforms the classical PA scheme for any value of  $D_1$  and in all the transmitted SNR region. Also, for fixed  $\frac{P_{\max}}{N_0}$ , as  $D_1$  increases, the impact of IQI in the average achievable capacity become more severe, when the classical PA is employed. For example, for  $\frac{P_{\max}}{N_0} = 40$  dB and  $D_1 = 1$ , each UE's capacity equals 6.5 bits/sec/Hz, whereas, for the same  $\frac{P_{\max}}{N_0}$  value and  $D_1 = 3$ , each UE's capacity is 2.5 bits/sec/Hz. Moreover, we observe that as  $D_1$  increases the effectiveness of the proposed PA scheme increases. For instance, for  $\frac{P_{\max}}{N_0} = 40$  dB, the use of the proposed PA scheme results to 24.5%, 64.9% and 131.7% increase of the average UE's capacity for  $D_1 = 1$ ,  $D_1 = 2$  and  $D_1 = 3$ , respectively. This reveals that the proposed PA scheme provides even larger gain as compared to classic PA, when the UEs have different channel qualities.

## REFERENCES

- [1] T. Schenk, *RF Imperfections in High-Rate Wireless Systems*. The Netherlands: Springer, 2008.
- [2] T. T. Duy, T. Duong, D. Benevides da Costa, V. N. Q. Bao, and M. Elkashlan, "Proactive relay selection with joint impact of hard-

- ware impairment and co-channel interference,” *IEEE Trans. Commun.*, vol. 63, no. 5, pp. 1594–1606, May 2015.
- [3] A.-A. A. Boulogeorgos, N. Chatzidiamantis, G. K. Karagiannidis, and L. Georgiadis, “Energy detection under RF impairments for cognitive radio,” in *Proc. IEEE International Conference on Communications - Workshop on Cooperative and Cognitive Networks (ICC - CoCoNet)*, London, United Kingdom, Jun. 2015.
- [4] A.-A. A. Boulogeorgos, H. Bany Salameh, and G. K. Karagiannidis, “On the effects of I/Q imbalance on sensing performance in Full-Duplex cognitive radios,” in *IEEE Wireless Communications and Networking Conference WS 8: IEEE WCNC’2016 International Workshop on Smart Spectrum (IWSS) (IEEEWCNC2016-IWSS)*, Doha, Qatar, Apr. 2016.
- [5] A.-A. A. Boulogeorgos, P. C. Sofotasios, B. Selim, S. Muhaidat, G. K. Karagiannidis, and M. Valkama, “Effects of RF impairments in communications over cascaded fading channels,” *IEEE Trans. Veh. Technol.*, vol. PP, no. 99, 2016.
- [6] A. Gokceoglu, S. Dikmese, M. Valkama, and M. Renfors, “Energy Detection under I/Q Imbalance with Single- and Multi-Channel Direct-Conversion Receiver: Analysis and Mitigation,” *IEEE J. Sel. Areas Commun.*, vol. 32, no. 3, pp. 411–424, March 2014.
- [7] A. A. Boulogeorgos, H. B. Salameh, and G. Karagiannidis, “Spectrum sensing in full-duplex cognitive radio networks under hardware imperfections,” *IEEE Trans. Veh. Technol.*, vol. PP, no. 99, pp. 1–1, 2016.
- [8] M. Mokhtar, A.-A. A. Boulogeorgos, G. K. Karagiannidis, and N. Al-Dhahir, “OFDM opportunistic relaying under joint transmit/receive I/Q imbalance,” *IEEE Trans. Commun.*, vol. 62, no. 5, pp. 1458–1468, May 2014.
- [9] O. Ozdemir, R. Hamila, and N. Al-Dhahir, “Exact average OFDM subcarrier SINR analysis under joint transmit-receive I/Q imbalance,” *IEEE Trans. Veh. Technol.*, vol. 63, no. 8, pp. 4125–4130, Oct. 2014.
- [10] —, “I/Q imbalance in multiple beamforming OFDM transceivers: SINR analysis and digital baseband compensation,” *IEEE Trans. Commun.*, vol. 61, no. 5, pp. 1914–1925, May 2013.
- [11] A. Hakkarainen, J. Werner, K. Dandekar, and M. Valkama, “Analysis and augmented spatial processing for uplink OFDMA MU-MIMO receiver with transceiver I/Q imbalance and external interference,” *IEEE Trans. Wireless Commun.*, vol. PP, no. 99, pp. 1–1, Jan. 2016.
- [12] Y. Yoshida, K. Hayashi, H. Sakai, and W. Bocquet, “Analysis and compensation of transmitter IQ imbalances in OFDMA and SC-FDMA systems,” *IEEE Trans. Signal Process.*, vol. 57, no. 8, pp. 3119–3129, Aug. 2009.
- [13] Y. Tsai, C.-P. Yen, and X. Wang, “Blind frequency-dependent I/Q imbalance compensation for direct-conversion receivers,” *IEEE Trans. Wireless Commun.*, vol. 9, no. 6, pp. 1976–1986, Jun. 2010.
- [14] H. Lin and K. Yamashita, “Time domain blind I/Q imbalance compensation based on real-valued filter,” *IEEE Trans. Wireless Commun.*, vol. 11, no. 12, pp. 4342–4350, Dec. 2012.
- [15] Z. Zhu, X. Huang, and H. Leung, “Blind compensation of frequency-dependent I/Q imbalance in direct conversion OFDM receivers,” *IEEE Commun. Lett.*, vol. 17, no. 2, pp. 297–300, February 2013.
- [16] A.-A. A. Boulogeorgos, V. M. Kapinas, R. Schober, and G. K. Karagiannidis, “I/Q-imbalance self-interference coordination,” *IEEE Trans. Wireless Commun.*, vol. PP, no. 99, pp. 1–1, 2016.
- [17] A.-A. A. Boulogeorgos, N. D. Chatzidiamantis, and G. K. Karagiannidis, “Energy detection spectrum sensing under RF imperfections,” *IEEE Trans. Commun.*, vol. 64, no. 7, pp. 2754–2766, Jul. 2016.
- [18] A.-A. A. Boulogeorgos, Karas, and G. K. Karagiannidis, “How much does I/Q imbalance affect secrecy capacity?” *IEEE Commun. Lett.*, vol. 20, no. 7, pp. 1305–1308, Jul. 2016.
- [19] B. Narasimhan, D. Wang, S. Narayanan, H. Minn, and N. Al-Dhahir, “Digital compensation of frequency-dependent joint Tx/Rx I/Q imbalance in OFDM systems under high mobility,” *IEEE J. Sel. Topics Signal Process.*, vol. 3, no. 3, pp. 405–417, JUN 2009.
- [20] C. Sun, X. Gao, S. Jin, M. Matthaiou, Z. Ding, and C. Xiao, “Beam division multiple access transmission for massive MIMO communications,” *IEEE Trans. Commun.*, vol. 63, no. 6, pp. 2170–2184, Jun. 2015.
- [21] C. Guo, B. Liao, L. Huang, X. Lin, and J. Zhang, “On Convexity of Fairness-Aware Energy-Efficient Power Allocation in Spectrum-Sharing Networks,” *IEEE Commun. Letters*, vol. 20, no. 3, pp. 534–537, Mar. 2016.
- [22] S. Boyd and L. Vandenberghe, *Convex Optimization*. Cambridge University Press, 2009.
- [23] P. D. Diamantoulakis, K. N. Pappi, G. K. Karagiannidis, and H. V. Poor, “Autonomous Energy Harvesting Base Stations With Minimum Storage Requirements,” *IEEE Wireless Commun. Lett.*, vol. 4, no. 3, pp. 265–268, Jun. 2015.
- [24] P. D. Diamantoulakis, K. N. Pappi, S. Muhaidat, G. K. Karagiannidis, and T. Khattab, “Underlay cognitive radio: What is the impact of carrier aggregation and relaying on throughput?” in *IEEE Wireless Communications and Networking Conference*, Doha, Qatar, Apr. 2016, pp. 1–6.
- [25] J. Li, M. Matthaiou, and T. Svensson, “I/Q imbalance in two-way AF relaying,” *IEEE Trans. Commun.*, vol. 62, no. 7, pp. 2271–2285, Jul. 2014.